ELSEVIER

Journal of Power Sources 112 (2002) 162–173

JOURNAL OF POWER SOURCES

www.elsevier.com/locate/jpowsour

Design and analysis of aluminum/air battery system for electric vehicles

Shaohua Yang, Harold Knickle*

Department of Chemical Engineering, University of Rhode Island, Kingston, RI 02881, USA

Received 6 April 2002; accepted 14 June 2002

Abstract

Aluminum (Al)/air batteries have the potential to be used to produce power to operate cars and other vehicles. These batteries might be important on a long-term interim basis as the world passes through the transition from gasoline cars to hydrogen fuel cell cars. The Al/air battery system can generate enough energy and power for driving ranges and acceleration similar to gasoline powered cars.

From our design analysis, it can be seen that the cost of aluminum as an anode can be as low as US$ 1.1/kg as long as the reaction product is recycled. The total fuel efficiency during the cycle process in Al/air electric vehicles (EVs) can be 15% (present stage) or 20% (projected) comparable to that of internal combustion engine vehicles (ICEs) (13%). The design battery energy density is 1300 Wh/kg (present) or 2000 Wh/kg (projected). The cost of battery system chosen to evaluate is US$ 30/kW (present) or US$ 29/kW (projected).

Al/air EVs life-cycle analysis was conducted and compared to lead/acid and nickel metal hydride (NiMH) EVs. Only the Al/air EVs can be projected to have a travel range comparable to ICEs. From this analysis, Al/air EVs are the most promising candidates compared to ICEs in terms of travel range, purchase price, fuel cost, and life-cycle cost.

Keywords: Aluminum/air batteries; Life-cycle analysis; Electric vehicles; Cost analysis

1. Introduction

The Al/air battery system has a high theoretical voltage (2.7 V), high theoretical energy density (8.1 kWh/kg-Al), low cost, an environmentally benign and recyclable product. It turns out to be a promising system for EVs. The Al/air yields energy densities that exceed many other couples (Table 1) [1,2].

Al/air batteries have the potential to be used to produce power to operate cars and other vehicles. These batteries might be important on an interim basis as the world passes through the transition from gasoline cars to hydrogen fuel cells cars. The Al/air battery system could generate enough energy and power for driving ranges and acceleration similar to gasoline powered cars. The major problem in using this system is the low coulombic efficiency of aluminum in strong alkaline media resulting from its high corrosion rate (hydrogen evolution reaction) and high level of polarization during discharge. Use of high grade (99.99 or 99.999%) aluminum doped with other minor elements such as Ga, In, Sn, Mg, Pb, Hg, Mn, Tl, etc. [3–7] can reduce corrosion but increases the material cost. To demonstrate the ability of this system for vehicle applications, the range and acceleration capability similar to internal combustion engine vehicles (ICEs) on an economically sound basis must be provided. Thus, the analysis and estimation of the performance, cost and efficiency of the fuel (aluminum anode), the batteries, and the vehicles powered by this system are all important parts of this study.

2. Fuel cost and efficiency

2.1. Fuel cost

The presence of certain impurities in aluminum can markedly affect the electrochemical behavior. For example, the corrosion rate is particularly sensitive to the concentration of iron [5]. Typically the anode uses aluminum of high purity 99.995 and 99.999% with small amount of other elements, usually in combinations as ternary or quaternary alloys to achieve activation and inhibition of corrosion. The production of aluminum, the cost of aluminum required by the Al/air battery system are reviewed and estimated in this section.

* Corresponding author. Tel.: +1-401-874-5984; fax: +1-401-782-1066.
E-mail address: knickle@egr.uri.edu (H. Knickle).

0378-7753/02/$ – see front matter
PII: S0378-7753(02)00370-1

Table 1
Comparison of electrochemical couples [1,2]

Couple	Theoretical open circuit voltage (V)	Gravimetric	
		Theoretical energy density (Wh/kg)	Actual energy density (Wh/kg)
Al/air	2.7	8140	300–500
$LiSOCl_2$	3.6	1462	374–440
AgZn	1.86	526	140–200
AgCd	1.4	318	70–100
PbAC	2.15	252	30–45
NiCd	1.35	244	40–51
NiMH	1.35	206	50
Li-ion	3.6	631	130
Zn/air	1.4	1050	200–300

2.1.1. Aluminum production process

In industry, extraction of aluminum metal takes places in three main stages—bauxite mining, alumina production by Bayer process, and alumina electrolysis (the Hall–Herout process). To get high purity aluminum (>99.99%) electric refining is needed [8].

2.1.1.1. Bauxite miming [9]. Bauxite is the principal ore of aluminum. Bauxite is mined by surface methods (open cast mining) in which the topsoil and overburden are removed by bulldozers and scrapers. The underlying bauxite, broken by explosives if necessary, is mined by front-endloaders, power shovels or hydraulic excavators. Sometimes the bauxite is crushed and washed to remove some of the clay and sand waste and then dried in rotary kilns. Other bauxites may just be crushed or dried. The ore is then loaded into trucks, railway cars, or onto conveyor belts, and transported to ships or refineries.

Bauxite consists of aluminum oxide, Al_2O_3, more or less hydrated and containing various impurities, such as iron oxide, aluminum silicate, titanium dioxide, quartz, and compounds of phosphorus and vanadium. The composition of bauxites used in the aluminum manufacture varies a great deal, but the variations generally fall within the limits shown in Table 2.

2.1.1.2. Alumina production. In nearly all commercial operations, alumina is extracted from the bauxite by the Bayer process. The Bayer process, discovered by Karl Bayer in 1888, is carried out entirely in the aqueous phase, taking advantage of the solubility equilibrium of the alumina hydrates in caustic soda solution, in accordance with one or the other of the following equations:

$$AlO{-}OH + NaOH \rightarrow NaAlO_2$$

$$Al(OH)_3 + NaOH \rightarrow NaAlO_2 + H_2O$$

The Bayer process consists of four stages [10]:

- *Digestion*—in which the finely ground bauxite is fed into a steam-heated unit called a digester, where it is mixed, under pressure, with a hot solution of caustic soda. The aluminum oxide of the bauxite and some of the silica react with the caustic soda forming a solution of sodium aluminate or green liquor and a precipitate of sodium aluminum silicate.
- *Clarification*—in which the green liquor or alumina-bearing solution is separated from the waste (the undissolved iron oxides and silica which were part of the original bauxite and now make up the sand and the red mud waste). This stage involves three steps: firstly, the coarse sand-sized waste is removed and washed to recover caustic soda; secondly, the red mud is separated out; and thirdly, the remaining green liquor is pumped through filters to remove any remaining impurities. The sand and mud are together pumped to residue lakes and the liquor is pumped to heat exchangers where it is cooled from 100 to 50–60 °C.
- *Precipitation*—in this stage, the alumina is precipitated from the liquor as crystals of alumina hydrate. To do this, the green liquor solution is mixed in the tall precipitator vessels with small amounts of fine crystalline alumina, which stimulates the precipitation of solid alumina hydrate, as the solution cools. As the reaction is slow and limited, it takes 50–80 h to obtain the desired degree of precipitation. When completed, the solid alumina hydrate is passed onto the next stage and the remaining liquor, which contains caustic soda and some alumina, goes back to the digesters.
- *Calcination*—in the final stage, the alumina hydrate is washed to remove any remaining liquor and dried. Finally, it is heated to about 1000 °C to drive off the water of crystallization, leaving the alumina, which is a dry, pure, sandy material.

The physical properties of this alumina, characterized by its particle size and degree of calcination, are important to the user. One such property is its content of residual combined water and absorbed water. Furthermore, the alumina should be as pure as possible. Alumina of good quality has the characteristics shown in Table 3.

2.1.1.3. Electrolysis. All commercial production of aluminum is based on the Hall–Heroult process in which the aluminum and oxygen in the alumina are separated by electrolysis. This consists of passing an electric current through a molten solution of alumina and natural or

Table 2
Typical composition of bauxites for aluminum manufacture [8]

Composition	Percentage
H_2O, combined	12–30
A_2O_3, total	40–60
SiO_2, free and combined	1–15
Fe_2O_3	7–30
TiO_2	3–4
F, P_2O_5, V_2O_5, and others	0.05–0.2

Table 3
Composition of a good alumina [8]

Composition	Percentage
H_2O, combined (loss on calcination)	0.05–0.15
H_2O, adsorbed (loss at 110 °C)	0.20–0.50
SiO_2	0.005–0.015
Fe_2O_3	0.005–0.020
TiO_2	0.004–0.005
P_2O_5	<0.002
V_2O_5	<0.001
ZnO	<0.010
Na_2O	0.40–0.80

Table 5
Comparable cost of aluminum production in 2001 [11]

Company	Cost of production (US$/kg)
Kaiser (USA)	1.32
Alcoa (USA)	1.25
Reynolds (USA)	1.19
Alumax (USA)	1.18
Alcan (Canada)	1.11
VAW (Germany)	1.30
Nalco (India)	0.90
World average	1.25

synthetic cryolite (sodium aluminum fluoride). The molten solution is contained in reduction cells or pots which are lined at the bottom with carbon (the cathode) and are connected in an electric series called a potline. Inserted into the top of each pot are carbon anodes, the bottoms of which are immersed in the molten solution.

The passage of an electric current causes the oxygen from the alumina to combine with the carbon dioxide gas. The remaining molten metallic aluminum collects at the cathode at the bottom of the pot. Periodically, it is siphoned off and transferred to large holding furnaces. Impurities are removed, alloying elements added and the molten aluminum is cast into ingots. The material and energy consummations are listed in Table 4 [8].

A good portion of the metallic impurities present in the raw materials, especially Fe, Si, Ti, V, and Mn, may also be found in the aluminum. That is why the raw materials should be prepared in as pure a state as possible. As a rule, the metal is 99.6–99.8% pure.

The cost of aluminum (99.9% grade) can be estimated as following:

$$\text{aluminum (99.9\% grade) cost} = \text{alumina cost} + \text{electricity cost} + \text{anode material cost} + \text{cryolite cost}.$$

From Table 4, the electricity cost is US$ 0.06/kWh in the USA and the production cost of alumina/kg-metal is about US$ 0.30 [11].

Total cost of aluminum/kg is about US$ $((0.06 \times 15)+0.30) = $ US$ 1.20 (excluding the cost of anode material and cryolite); this value approximately equals the cost listed in Table 5 (world wide average US$ 1.25/kg-metal).

Table 4
Material and energy consumption of production for 1 kg of aluminum (99.9%) [8]

Material and energy	
Alumina (kg)	1.9
Anode material (kg)	0.45
Cryolite (kg)	0.07
Energy to produce 99.9% Al (kWh/kg)	15

2.1.1.4. Electrolytic refining [8]. The Hall–Herout process cannot ensure purity higher than about 99.9%; other techniques were therefore required when an extremely high purity was desired.

The principle of electrolytic refining, as described by Betts in 1905, is still in use today. It is based on the use of a bath containing three layers. The bottom of the cell, which is a carbon anode, as well as its sides which are nonconductors of electricity, are covered with a dense layer of aluminum–copper alloy. Upon this layer rests another layer of electrolyte, which contains aluminum cations. The density of this layer is slightly below that of the aluminum–copper alloy but above that of aluminum itself. Finally, covering these is a third layer, which is pure refined serving as the cathode. The metal may attain a purity of 99.995%. The material and energy consummations are shown in Table 6 [8].

The cost of 1 kg of refined aluminum can be estimated as following:

$$\text{refined aluminum cost} = \text{aluminum cost (99.9\% grade)} + \text{electricity cost} + \text{other material costs}.$$

According to Table 6, aluminum (99.9% grade) cost is US$ 1.25/kg-Al and the electricity cost to refine 1 kg of aluminum is US$ $(18 \times 0.06) = $ US$ 1.08.

$$\text{Total cost of refined aluminum (99.995\% grade)} = \text{US\$}\,(1.25 + 1.08) = \text{US\$}\,2.33/\text{kg-metal}.$$

2.1.2. Recycled fuel cost estimation

In an Al/air battery system, the anode used is of high purity (99.995%) with a small amount of alloy elements that

Table 6
Material and energy consumption for production of 1 kg of refined aluminum (99.99%) [8]

Material and energy	
Aluminum (99.9%) (kg)	1
Bath material (kg)	0.06
Graphite (kg)	0.02
Energy to produce 99.99% Al (kWh/kg)	18

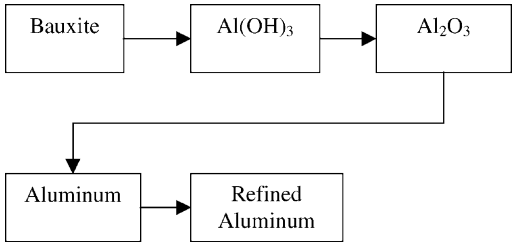

Fig. 1. Refined aluminum production process.

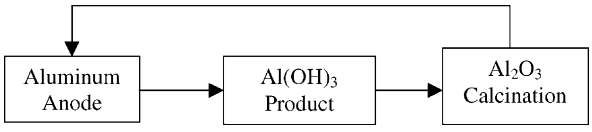

Fig. 2. Aluminum recycling process in an Al/air EVs for computation of theoretical fuel energy cycle efficiency.

have positive effects on the performance of the anode, i.e. high open circuit potential and low corrosion. Use of the battery produces $Al(OH)_3$. $Al(OH)_3$ is then calcined into Al_2O_3 followed by electrolysis to Al (99.995%). We assume the impurities such as Fe, Si and other harmful elements are not added during this stage. Energy and material consumption is considerably reduced through this recycle process.

For comparison, the refining of aluminum from bauxite is shown in Fig. 1 in a very simplified form. The aluminum recycle process from the chemical product of a battery system is shown in three steps in Fig. 2. The cost for recycling aluminum consists of the cost of electrolysis and the cost of calcination. If the energy consumption is still 15 kWh/kg-Al for electrolysis of alumina, the cost of electrolysis is approximately US$ 0.90/kg-Al (excluding other material cost, labor cost etc.). The cost of calcinations in the recycle process is about 22% (assuming that this is equal to the energy requirement of calcination divided by that of electrolysis; see Section 2.2 for energy requirements of each process) that of calcination or US$ 0.20. So the total cost of the anode with recycle is about US$ 1.10/kg-Al. The cost of the anode with and without recycling is listed in Table 7.

2.2. Fuel efficiency (calculation basis: 1 mol Al)

When placed in the battery, aluminum reacts with oxygen from the air and with water in the electrolyte to provide power for the EVs. The product of the discharge reaction is

Table 7
Estimated cost of anode materials from electrolytic refining and recycled from Al/air EVs

Anode material	Cost (US$/kg)
Refined aluminum (from mine)	2.33
Recycled aluminum	1.10

Table 8
Thermodynamic properties of various chemicals [13]

Element or compound	Formation energy, ΔH_f° (kJ/mol)
Al(s)	0
$Al(OH)_3$	−1272.8[a]
Al_2O_3	−1669.8
H_2O	−241.8
O_2	0

[a] Source: [14].

$NaAlO_2$ which is precipitated in the form of hydrargillite, $Al_2O_3{\cdot}3H_2O$ or $Al(OH)_3$. This is heated and decomposed into Al_2O_3. The Al_2O_3 is regenerated to aluminum metal by electrolysis.

In our calculation of fuel energy cycle efficiency, our basis is 1 mol of aluminum. Assuming complete battery energy discharge is 80% (20% unused aluminum). The heats of formation used in our calculations are listed in Table 8. The EVs aluminum fuel cycle is shown in Fig. 3.

2.2.1. EVs aluminum fuel cycle energy balance components

There are four components of the fuel cycle energy balance of the EVs. These include the usable energy contained in the aluminum anodes, the heat of reaction from $Al(OH)_3$ to Al_2O_3, the heat of reaction from Al_2O_3 to Al, and unused aluminum reformed to anode plates. These are depicted in Fig. 3.

1. Energy contained in used aluminum: an optimistic value for the useable energy density of aluminum is estimated as 564 kJ/mol (72% of theoretical value of 783 kJ/mol [12]). Thus, 0.8 mol aluminum has useable energy of 451 kJ.
2. The heat of reaction from $Al(OH)_3$ to Al_2O_3: the reaction is

$$Al(OH)_3(s) \rightarrow \tfrac{1}{2}Al_2O_3(s) + \tfrac{3}{2}H_2O(g) + \Delta H^\circ$$

The heat of reaction from the formation energies for the above reaction is

$$\Delta H^\circ = \tfrac{1}{2}(-1169.8) + \tfrac{3}{2}(-241.8) - (-1272.8) = 325.2\,\text{kJ/mol}.$$

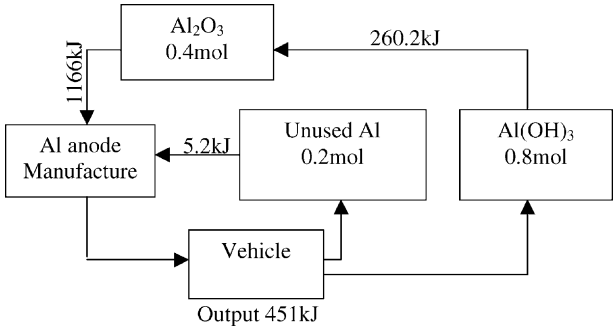

Fig. 3. Fuel cycle of Al/air EVs: cycle used for computation of fuel energy cycle efficiency.

Decomposition of 0.8 mol $Al(OH)_3$ needs 260.2 kJ energy to decompose into 0.4 mol of Al_2O_3.

3. The heat of reaction from Al_2O_3 to Al:

$$Al_2O_3 \rightarrow 2Al + \tfrac{3}{2}O_2$$

The heat of above reaction is 1669.8 kJ/mol. Electrolyzing 0.4 mol Al_2O_3 needs 667.92 kJ in theory to produce 0.8 mol of aluminum. Actually [8] industry uses 15 kWh to produce 1 kg of aluminum. Therefore, industry would use 1166 kJ to produce 0.8 mol aluminum.

4. Unused aluminum to anode plate: aluminum requires only 26 kJ/mol to melt. So the energy requirement of melting unused 0.2 mol Al is 5.2 kJ.

2.2.2. Fuel energy efficiency estimation with recycle

2.2.2.1. Theoretical efficiency. The theoretical energy density of Al is 783 kJ/mol-Al. For a theoretical cycle for 1 mol aluminum consumed, the total theoretical energy required is made up from the energy used in calcinations (325.2 kJ) and the energy used in electrolysis (834.9 kJ). The total theoretical energy require is 1160.1 kJ. Thus, the energy efficiency of the recycle process is (783/(1160.1 × 100)) 67.5% (see Fig. 2). This is the maximum possible efficiency of the recycle process.

2.2.2.2. Actual efficiency. From Fig. 3, the actual total energy required for recycling is made up of the three components the previous section (260.2 + 1166 + 5.2). The total energy used is 1431.4 kJ. The energy efficiency for regeneration and recycle is the energy produced from the battery (451 kJ) divided by the energy required for recycle (1431 kJ) or 31.5%.

A battery efficiency of 0.8, and motor/transmission efficiency of 0.8, results in the EVs operating efficiency of (0.8 × 0.8 × 100) 64%. These factors result in an actual total cycle efficiency including recycle for the Al/air EVs in the steady state of (0.315 × 0.64) 20.2%.

From these efficiency calculations we construct Fig. 4. It must be noted that, here the anode energy density of 564 kJ/mol (5.8 kWh/kg-Al, projected techniques; see Section 3) is assumed. If the anode energy density of 418 kJ/mol (4.3 kWh/kg-Al, present techniques; see Section 3) is used in the calculation, the fuel energy efficiency in this cycle is about 15%.

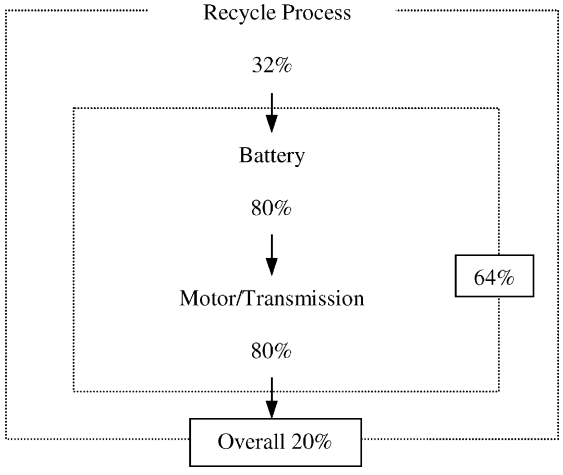

Fig. 4. Fuel energy cycle efficiency in an Al/air EVs.

3. Battery system analysis

3.1. Cell performance model

The mathematical model of the Al/air cell provides the means to simulate the electrical characteristics of the Al/air battery during changing operating conditions. Cell characteristics are also a key determinant of the physical characteristics of the Al/air battery and its associated vehicle. The power and energy characteristics of the cell principally determine total battery mass (BM), which greatly influence total vehicle mass (VM) and cost [12].

Voltage and current data from Behrin et al. [12] were modeled with a cubic polynomial using

$$V = a + b(ir) + c(ir)^2 + d(ir)^3 \tag{1}$$

where $a = V_0$; V_0 is open circuit potential of the cell; r is the resistivity of electrolyte.

The parasitic current is modeled as follows:

$$i_p = i_{p0} + mi \tag{2}$$

Eq. (1) can be rewritten as

$$\frac{V}{V_0} = 1 + \left(\frac{b}{a}\right)(ir) + \left(\frac{c}{a}\right)(ir)^2 + \left(\frac{d}{a}\right)(ir)^3 \tag{3}$$

The power density is

$$P_d = Vi \tag{4}$$

The energy density is

$$E = \frac{q_0 P_d}{(i + i_p)} \tag{5}$$

where E is the energy density (kWh/kg-Al); $q_0 = F/\text{Weq} = 2.98$ (kAh/kgeq); $F = 96487$ (kC/kgeq); Weq = 9 (kg-Al/kgeq).

Combining Eqs. (4) and (5) gives

$$E_d = \frac{q_0 Vi}{(i + i_p)} \tag{6}$$

or,

$$E_d = q_0 V_0 \left(\frac{V}{V_0}\right)\left[\frac{i}{i + i_p}\right] \tag{6}\prime$$

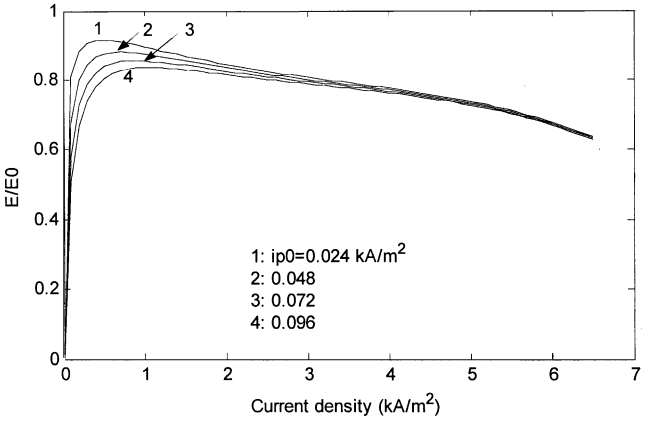

Fig. 5. Effects of corrosion current density on the energy density of anode material.

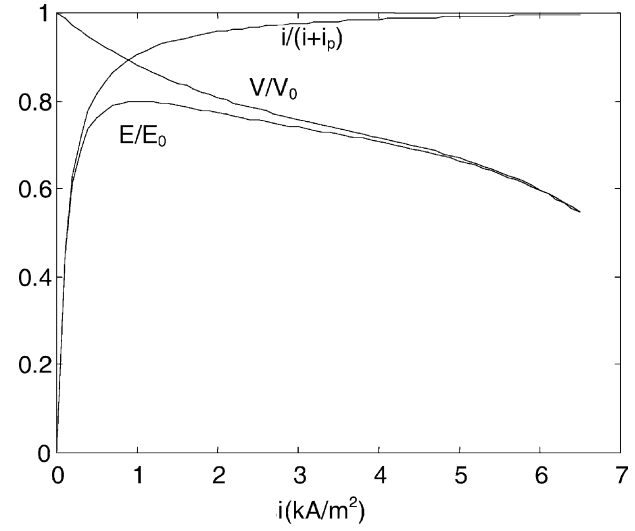

Fig. 6. Present voltage and energy density characteristics for an Al/air cell with an inter-electrode gap of 2 mm, and 1.0 M aluminate concentration at 60 °C.

Table 9
Parameters for calculating present and projected Al/air battery characteristics at 1.0 M aluminate, 4N NaOH and 60 °C [12] (see Eqs. (1) and (2))

Parameters	Present	Projected
a (V)	1.8	2.2
b (mm)	−13.95	−13.95
c (mm^2/V)	152.6	152.6
d (mm^3/V^2)	−767.4	−767.4
r (Ω m)	0.1866	0.1866
m	−0.015	−0.015
i_{p0} (kA/m^2)	0.100	0.024

Let $E_{d0} = q_0 V_0$, then Eq. (6)′ becomes

$$\frac{E_d}{E_{d0}} = \left(\frac{V}{V_0}\right)\left[\frac{i}{(i+i_p)}\right] \quad (6)''$$

3.1.1. Current and projected Al/air battery characteristics

The key present stage characteristics are parasitic current, present stage power density, energy density, and voltage. The parasitic current (corrosion current) has a great effect on the energy density of the anode as shown in Fig. 5. The effects of the present stage power density, energy density, and voltage are shown in Figs. 6–8 (Table 9) [12]. The present stage battery characteristics are based on Behrin et al. [12] so-called "near-term" characteristics, with slight modification. This modification is based on our experimental results and other authors' work [15–17]. From Fig. 8 the energy density is evaluated at a current density 2 kA/m^2 for normal operation.

The projected cell characteristics are similar to those given by Behrin et al. [12], the improved characteristics could be achieved by improving air cathodes, anodes and electrolytes. The projected characteristics of the cell are shown Figs. 9–11.

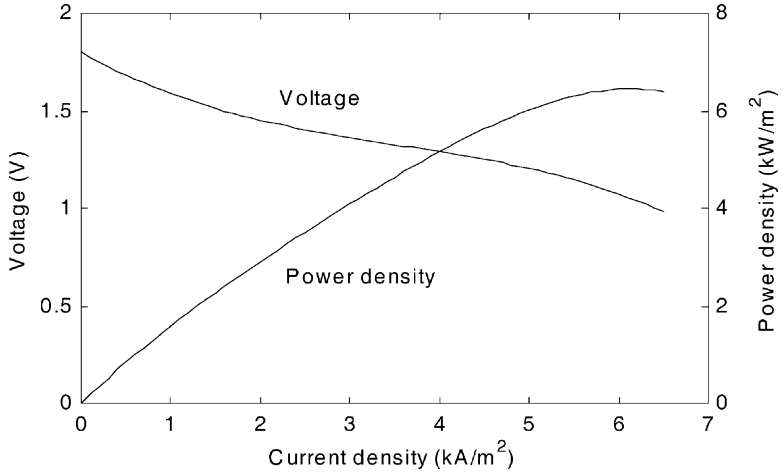

Fig. 7. Present voltage and power density characteristics for an Al/air cell with inter-electrode gap of 2 mm, and 1.0 M aluminate concentration at 60 °C.

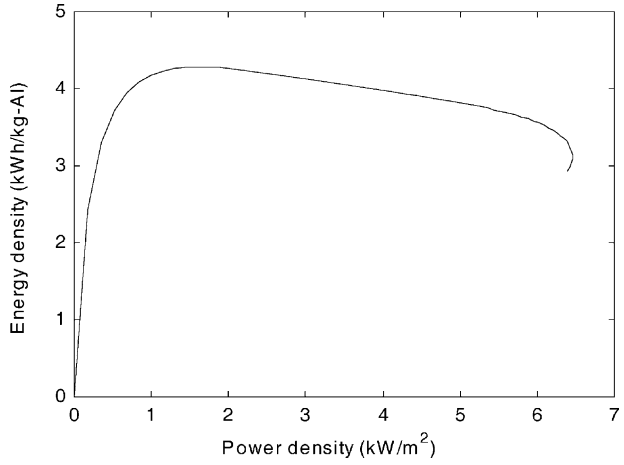

Fig. 8. Energy density for the present stage Al/air cell at 60 °C.

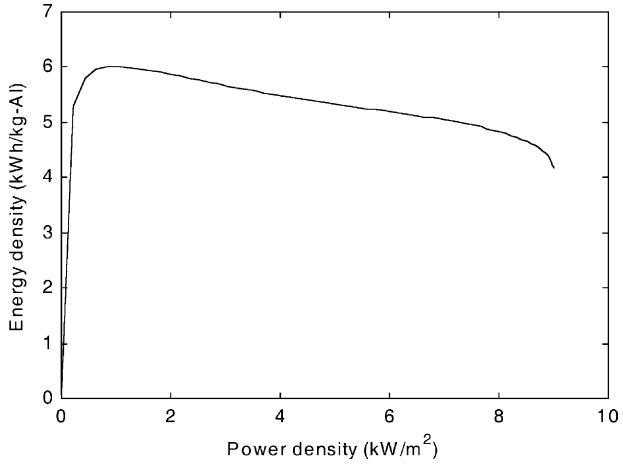

Fig. 11. Energy density for the projected Al/air cell characteristics at 60 °C.

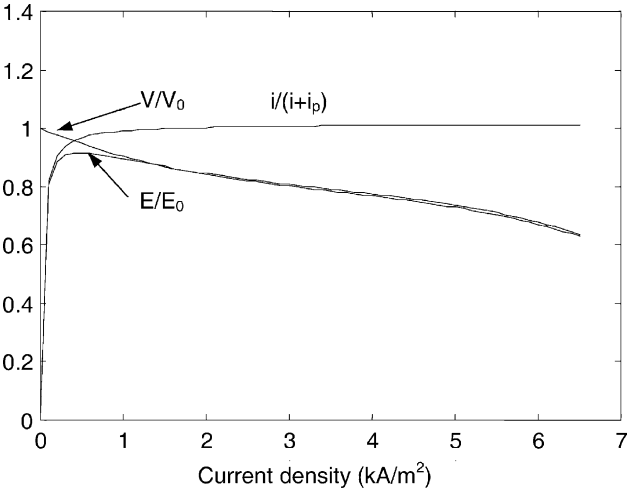

Fig. 9. Projected voltage and energy density characteristics for an Al/air cell with an inter-electrode gap of 2 mm, and 1.0 M aluminate concentration at 60 °C.

The resulted energy density, peak power (PP) density for present and projected characteristics are listed in Table 10.

3.2. Mass and volume of battery system analysis

3.2.1. Effect of power density and energy on mass and volume of battery system

If the peak power of the battery is 34.8 kW, anode mass is 82.9 kg and total number of cells 136 (two module with 68 cells each), we calculated the dependence of the mass and volume of the battery system on the peak power density and energy density of anode. From Fig. 12, it can be concluded that, an increase in both power density and energy density can considerably decrease both mass and volume of the battery system.

3.2.2. Mass distribution and volume of Al/air battery system

The mass distribution and volume of the Al/air battery system are shown in Figs. 13 and 14. It can be seen from

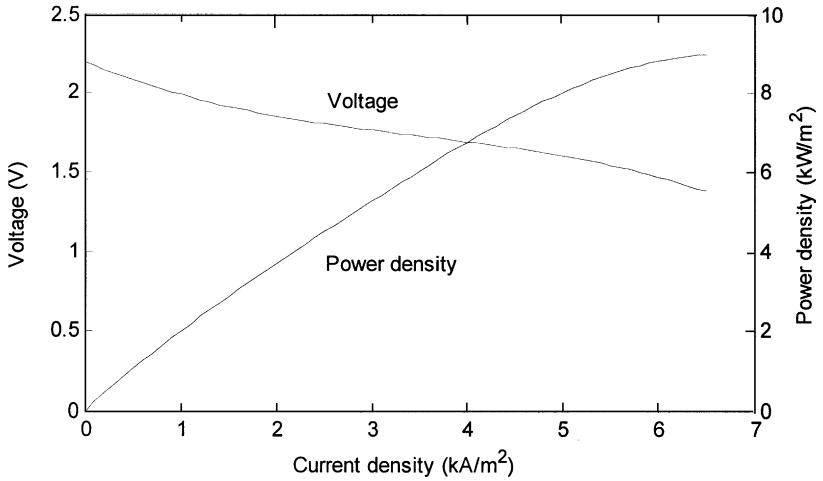

Fig. 10. Projected voltage and power density characteristics for an Al/air cell with inter-electrode gap of 2 mm, and 1.0 M aluminate concentration at 60 °C.

Table 10
Present and projected battery characteristics

Parameters	Present	Projected
E_d (kWh/kg-Al)	4.3	5.8
P_d (kW/m^2)	6.0	7.6

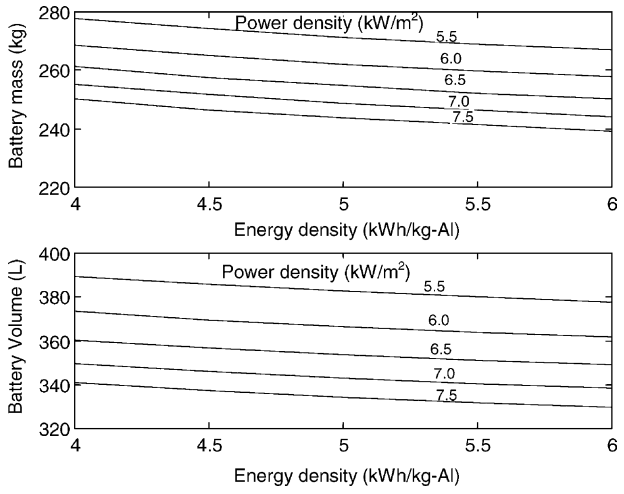

Fig. 12. Effect of power density on mass and volume of the battery system.

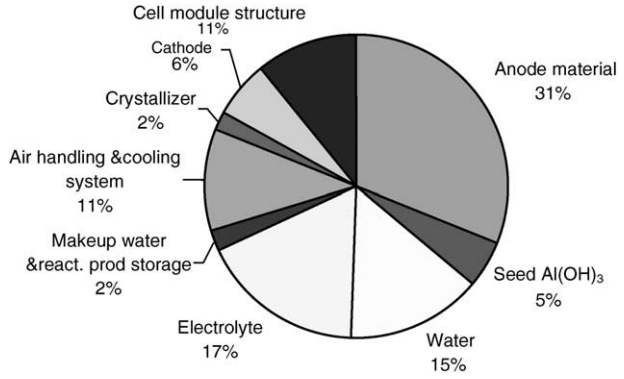

Fig. 13. Mass distribution of a fully fueled Al/air battery system (present). Peak power = 34.8 kW, total mass = 267 kg, total volume = 371 l.

Figs. 13 and 14 that, the mass of battery decreases 10% and volume decreases 11% due to the improved battery characteristics. And also, most of the battery system mass comes from the reactants. For the present characteristics, the reactants take up 67% of the total mass and for projected characteristics, the reactants take up 70% of the total mass.

From Figs. 13 and 14, the energy densities calculated are 1300 and 2000 Wh/kg for present and projected techniques respectively, these values are far larger than the values for Al/air system listed in Table 1.

3.2.3. Cost distribution of the battery system (in 2001 US$)

Cost and cost distribution of battery system are shown in Figs. 15 and 16 for both present and projected characteristics. The costs of the battery system with peak power

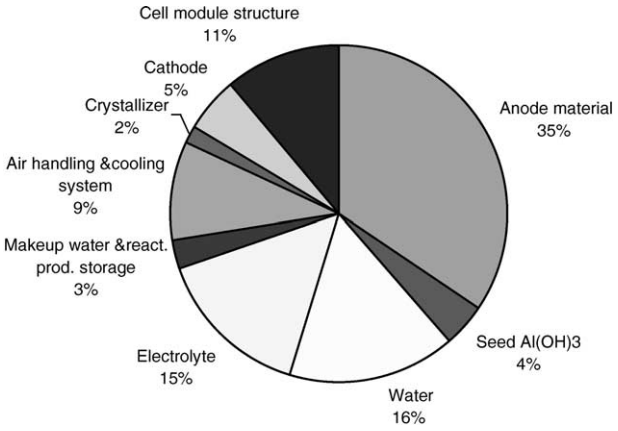

Fig. 14. Mass distribution of a fully fueled Al/air battery system (projected). Peak power = 34.8 kW, total mass = 240 kg, total volume = 329 l.

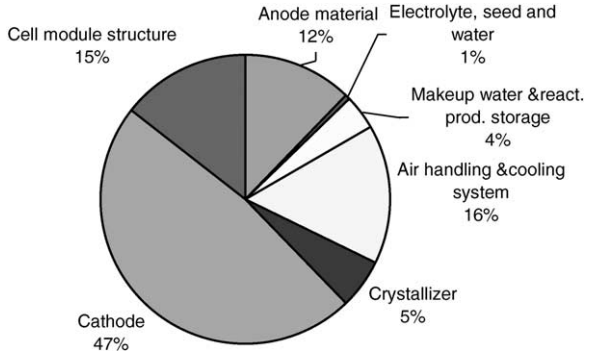

Fig. 15. Cost distribution of a fully fueled Al/air battery system (2001 US$) (present characteristics). Peak power = 34.8 kW, total cost = US$ 1120.

34.8 kW predicted are US$ 1019 or 32/kW (present) and US$ 1120 or 29/kW (projected), respectively. The cost can decrease 9% due to the improved characteristics. It can also be seen from both Figs. 15 and 16 that, the major cost items are the air cathode modules, which take up for approximately 50% of the total cost. In this calculation, the air cathode cost is US$ 100/m^2 is assumed (the cost of some of the current commercial air cathode is higher than

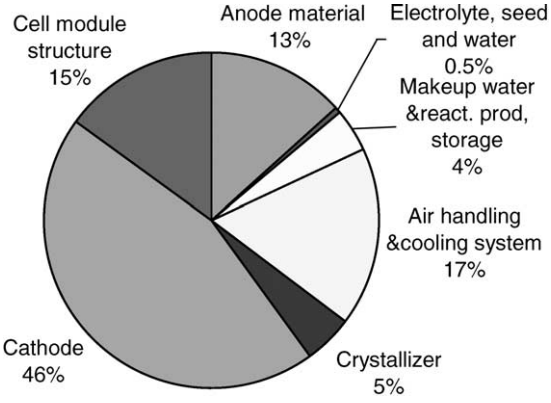

Fig. 16. Cost distribution of a fully fueled Al/air battery (2001 US$) (projected). Peak power = 34.8 kW, total cost = US$ 1019.

this value and are not used in our analysis). The cost of Al/air battery is much less than the cost of the present fuel cell stack (US$ 1219/kW) [18].

4. Life-cycle cost analysis of electric vehicles

Electric vehicle (EVs) have low emissions and are capable of using regeneratable energy. They are an alternative to conventional ICEs. Many battery technologies have been studied and appraised for EVs including lead/acid, zinc/air, nickel metal hydride (NiMH), nickel cadmium batteries [19–21]. The Al/air battery offers the potential of a very high energy density system [16]. There are few papers in the literature about the use of the Al/air battery system as a power source for EVs. Life-cycle energy and cost analysis calculations have been made using a cost program developed for estimating the life-cycle and operating costs of Al/air battery powered sub-compact cars.

4.1. Cost basis

An electrically powered passenger vehicle shares many common components with a conventional vehicle. The differences are mainly in the power train (engine and transmission group) and the fuel energy storage system, i.e. Al/air battery system. Both types have similar bodies and chassis components. Combining these similar components account for 78–80% of the total vehicle cost. Therefore, we base the EVs cost estimates mostly from available ICEs data and then make necessary adjustments for the differences in the hardware and system between the two for the remaining parts. Detailed cost allocation and calculation of ICEs (Table 11) were given by Vyas et al. [22]. Once the components unique to the EVs have been defined and their manufacturing cost assigned, it is possible to calculate the cost of the entire vehicle.

Table 11
Manufacturing cost allocation by group and subgroup for ICEs [22]

Vehicle group and subgroup	Share of vehicle cost (%)	
	Group	Subgroup
Body group	34.5	
Engine group	16.00	
Transmission group	4.75	
Chassis group	22.00	
Fuel storage		0.45
Others		21.55
Vehicle assembly	23.00	
Total	100.00	

4.2. Cost analysis model

The Al/air battery data and cost analysis were based on a modified battery physical model and cost program originally developed by Behrin et al. [12]. All the material cost is updated to 2001 using the chemical process cost index [23]. The peak power requirement of the traction motor was computed to meet an acceleration requirement of 0–96 km/h in about 20 s. The normal power (NP) used is calculated according to a mix of SAEJ1798 [24] and 96 km/h high way cruising. Once the peak power, normal power, range and

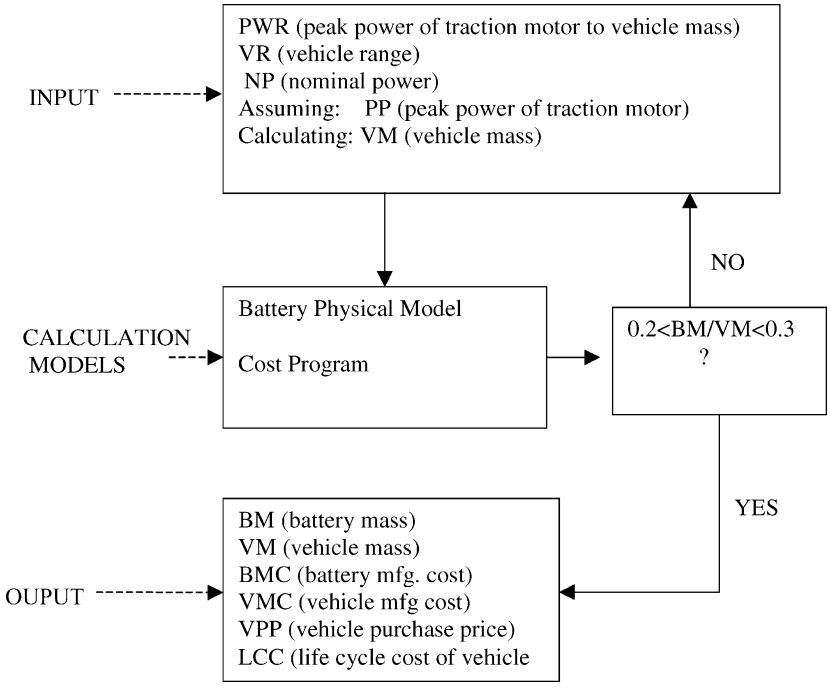

Fig. 17. Schematic of cost analysis procedure.

Table 12
Basic specifications of EVs analyzed

Vehicle characteristic	Al/air		Lead/acid[a]		NiMH[a]	
	Present	Projected	Initially	After 20 years	Initially	After 20 years
PWR (W/kg)[b]	33	33	33		33	33
Battery capacity (kWh)	204	204	19	12	32	23
Traction motor power (kW)	48	40	56	44	55	44
Battery mass (kg)	280	221	481	245	442	261
Vehicles mass (kg)	1280	1088	1571	1201	1525	1219
Estimated range (km)	400[c]	400[c]	122	98	212	192

[a] Data predicted for 2000 [22].
[b] PWR: traction motor peak power/(vehicle mass + 136 kg of payload).
[c] Battery has enough aluminum anode to have a range 1600 km requiring four stops for addition of water.

speed are assigned, the mass, volume and cost of the battery system can be calculated (assuming the battery system to the traction motor efficiency of 0.85).

The main choices in the power train design are dependent upon the type of motor and controller to use. We analyzed the production of electric traction motor and controls under a high volume production scenario. We assumed an induction motor in our cost analysis presented in this paper. The motor costs US$ 17/kW and the controller US$ 45.50/kW [22].

For the life-cycle cost analysis, the ICE car purchase price is set at US$ 15,500. The fuel economy for ICEs is about 30 mpg [25]. Both ICEs and EVs are assumed to have a life of 12 years and a range of 17,600 km per year. The total life-cycle cost for the EVs or ICEs are calculated by adding up the annualized initial user's cost fuel cost and non fueling cost such as maintenance cost, tire replacement cost, insurance cost, cathode replacement cost, and other cost. These are converted to annual cost/km.

4.3. Cost analysis procedures

The schematic flow diagram of Fig. 17 describes the main program for the EVs powered by the Al/air battery. The main input parameters are peak power of traction motor to vehicle mass (PWR), normal power, and by assuming the peak power of traction motor, we can calculate the vehicle mass. Other input parameters associated with vehicle and battery mass and cost calculation are not shown here, some of them are stated in previous paragraph and some are set as default parameters, such as energy density of aluminum anode, peak power/m^2 of the battery, concentration of electrolyte, and various material costs, etc. once the required parameters are set, then we can perform battery calculation and cost analysis using the battery physical model and cost program. The battery mass to vehicle mass ratio is confined to 0.2–0.3, which is generally accepted value. The output parameters are battery mass, vehicle mass, battery manufacture cost (BMC) and vehicle manufacture cost (VMC) and various cost related items.

4.4. Specifications and cost allocations of vehicles analyzed

Table 12 indicates the basic specifications of vehicles analyzed. The peak power to vehicle mass including 136 kg of payload is kept at about 33 W/kg. Compared with lead/acid and NiMH EVs. Al/air EVs have less vehicles mass, much higher battery capacity (at least 10 times that of lead/acid and 6 times that of NiMH). The projected improvement of Al/air battery characteristics is due to the improvements of aluminum anode energy density from 4.3 to 5.8 kWh/kg and battery peak power from 6.0 to 7.6 kW/m^2, thus the resulting vehicles mass is lowered without sacrifice of the battery capacity and vehicle range. The initial mass of the lead/acid and NiMH vehicles is quite heavy due to the initial high mass of the batteries of both these vehicles. The projected lead/acid and NiMH have battery mass comparable

Table 13
Cost allocation for EVs (%)

Vehicle cost component	Al/air		Lead/acid[a]		NiMH[a]	
	Present	Projected	Initially	After 20 years	Initially	After 20 years
Common components and assembly	55.3	58.6	57.5	79.4	33.6	62.8
EV power train	28.1	25.6	23.0	7.7	13.1	6.1
Battery pack	14.5	13.6	17.3	10.6	52.0	29.3
Subsystem premiums	2.0	2.2	2.2	2.3	1.3	1.8
Total	100.00	100.00	100.00	100.00	100.00	100.00

[a] Data predicted for 2000 [22].

Table 14
Cost ratios of Al/air, lead/acid, and NiMH EVs in comparison to ICEs

Items	Al/air		Lead/acid[a]	NiMH[a]
	Present	Projected		
Price ratio	1.3	1.25	1.25	1.9
Fuel cost ratio	1.35	1.01		
Life-cycle cost per km ratio	1.22	1.14	1.2	1.68
Estimated range	400[b]	400[b]	130	180

[a] Data predicted for 2000 [22].
[b] Battery has enough aluminum anodes to have a range 1600 km requiring four stops for addition of water.

(slightly less than) with aluminum/air, but sacrifice some of the battery capacity reducing the range of these vehicles. Also, only the projected Al/air battery EVs have a vehicle mass (1088 kg) similar to the average ICEs mass and a range (400 km) comparable with that of the ICEs.

Table 13 indicates the costs allocations of vehicle components for each type of EVs. Compared with ICEs, the Al/air EVs common components and assembly costs are assumed to be 55.3%. This is much less than that of ICEs at 78–80% due to the higher cost of the EV power train and battery pack. Compared with the lead/acid and NiMH EVs, the Al/air EVs power train cost decreases from 28.1 to 25.6%, a difference of only 2.5%, while the latter two types of EVs power train cost decreases from 23.0 to 7.7% and from 13.1 to 6.1%. In our calculation, we keep the cost of the power train of EVs constant, and in the lead/acid and NiMH EVs calculation (Vyas et al. [22]) the power train and battery pack cost are both projected to decrease.

4.5. Purchase price and life-cycle costs

Table 14 compares various cost ratios for the three EVs of Al/air, lead/acid and NiMH to those of ICEs. The calculated results for the actual purchase price and life-cycle cost are not shown in Table 14 but are summarized here. The purchase price for ICEs is US$ 15,500 and for that of the Al/air EVs is US$ 20,150 (present techniques) or US$ 19,300 (projected techniques). Fuel cost for ICEs is 3.1 cents/km and for Al/air EVs is 4.2 cents/km (present) or 3.2 cents/km (projected). Life-cycle cost per kilometer for ICEs is about 22.0 cents/km and for Al/air EVs is about 26.8 cents/km (present) or 25 cents/km (projected).

From the above results and Table 14, we can see that, the purchase price of Al/air EVs is 25–30% higher than the ICEs. This value is almost equal to that of lead/acid EVs, and is lower than that of NiMH EVs. At the present stage of development, fuel cost of Al/air EVs would be 35% higher than that of ICEs. But with the improvement of battery characteristics (projected battery aluminum anode characteristics), the fuel cost would decrease to a value comparable to that of ICEs. Life-cycle cost of Al/air EVs would be 14 and 22% higher than that of ICEs. These life-cycle costs are similar to lead/acid EVs and much lower than that of NiMH EVs.

5. Summary

The cost of aluminum as an anode can be as low as US$ 1.1/kg as long as the reaction product is recycled. The total fuel efficiency during the cycle process in an Al/air EVs can be 15% (present stage) or 20% (projected), comparable to that of ICEs. The battery energy density is 1300 Wh/kg (present) or 2000 Wh (projected), far better than other electrochemical couples shown in Table 1. The cost of the battery system chosen is US$ 30/kW (present) or US$ 29/kW (projected), far less than the present hydrogen fuel cell stack (US$ 1219/kW).

We have conducted Al/air EVs life-cycle analysis and compared the results with that of lead/acid and NiMH EVs. Only the Al/air vehicles can be projected to have a travel range comparable to ICEs. The purchase price of aluminum/air EVs would cost 25–30% more than the present ICEs. With the decrease in cost of the power train, the purchase price will likely drop farther. The fuel cost of the Al/air EVs at present is 35% higher than that of ICEs. But with improvement in battery characteristics, the fuel cost would fall to a level almost equal to that of ICEs. The life-cycle cost of Al/air EVs is 14% (projected) and 22% (present) higher than that of ICEs. Only the lead/acid EVs life-cycle cost is comparable to Al/air EVs life-cycle cost while the NiMH EVs is the highest.

From this analysis Al/air EVs are more promising candidates, than lead/acid or NiMH, for replacement of ICEs considering travel range, purchase price, fuel cost, and life-cycle cost.

Acknowledgements

This project is partially funded through the RI State Energy Office.

References

[1] D. Linden, Handbook of Batteries and Fuel Cells, NAVSEA Battery Document (NAVSEA-AH-300), 1st ed., McGraw-Hill, New York, 1993.
[2] T.A. Dougherty, A.P. Karpinski, J.H. Stannard, W. Halliop, S. Warner, Aluminum–air: status of technology and applications, in: Proceedings of the Conference on Intersociety Energy Conversion Engineering, IEEE V2 (1996) 1176–1180.
[3] A.R. Despic, D.M. Drazic, P.M. Milovan, Electrochemically active aluminum alloy, the method of its preparation and use, US Patent 4,098,606 (1978).
[4] B.B. Jovanovic, A.R. Despic, D.M. Drazic, Electrochemically active aluminum alloy and composite, US Patent 4,288,500 (1981).
[5] P.W. Jeffrey, W. Halliop, F.N. Smith, Aluminum anode alloy, US Patent 451,086 (1988).
[6] J.A. Hunter, G.M. Scamans, W.B. O'Callaghan, Aluminium batteries, Alcan International Limited, Montreal, CA, US Patent 4,942,100 (1990).
[7] Z. Solomon, C.C. Norman, R.M. Mazgaj, Aluminum-consuming fluidized-bed anodes, J. Electrochem. Soc. 137 (6) (1990) 1851–1856.

[8] F.M. Herman, J.M. John Jr., F.O. Donald, S. Anthony (Eds.), Aluminum and Aluminum Alloys, Encyclopedia of Chemical Technology, 2nd ed., vol. 1, Wiley, New York, 1963.
[9] http://www.eaa.net/pages/material/production.html, 2001.
[10] http://www.minerals.org.au/pages/page3_34.asp, 2001.
[11] http://www.indianinfoline.com/sect/alum/ch07.html, 2001.
[12] E. Behrin, R.L. Wood, J.D. Salisbury, D.J. Whisler, C.L. Hudson, Design Analysis of an Aluminum–Air Battery for Vehicle Operations, Transport system Research, Lawrence Livermore Laboratory, 1983.
[13] M.B. Gordon, Physical Chemistry, 3rd ed., McGraw-Hill, New York, 1973, pp. 779–784.
[14] http://www.eiu.edu/∼eiuchem/GenChem/downloads/tutorial8.pdf, 2001.
[15] D.W. Gibbons, E.J. Rudd, Development of aluminum/air batteries for propulsion applications, in: Proceedings of the 28th Conference on Intersociety Energy Conversion Engineering, vol. 1, Atlanta, 8–13 August 1993.
[16] R.P. Hamlen, W.H. Hoge, J.A. Hunter, W.B. O'Callaghan, Applications of aluminum–air batteries, IEEE Aerosp. Electron. Syst. Mag. 6 (10) (1991) 11–14.
[17] M.L. Doche, F. Novel-Cattin, R. Durand, J.J. Rameau, Characterization of different grades of aluminum anodes for aluminum/air batteries, J. Power Sources 65 (1/2) (1997) 197–205.
[18] K.S. Jeong, B.S. Oh, Fuel economy and life-cycle cost analysis of a fuel hybrid vehicle, J. Power Sources 5 (1) (2002) 58–65.
[19] A.K. Shukla, A.S. Arico, V. Antonucci, An appraisal of electric automobile power sources, Renewable Sustainable Energy Rev. 5 (2) (2001) 137–155.
[20] I. Rade, B.A. Andersson, Requirement for metals of electric vehicle batteries, J. Power Sources 93 (1/2) (2001) 55–71.
[21] R.F. Nelson, Power requirement for batteries in hybrid electric vehicles, J. Power Sources 91 (1) (2000) 2–26.
[22] A. Vyas, R. Cuenca, L. Gaines, An assessment of electric vehicle life-cycle costs to consumers, in: Proceedings of the Conference and Exposition on Total Life-Cycle, Argonne National Laboratory, Graz, Austria, 1–3 December 1998, SAE Technical Paper Series 982182.
[23] Economic Indicators, M&S Equipment Cost Index, Chemical Engineering, July 1981 to May 1982 and May 2001.
[24] Recommended practice for performance rating of electric vehicle battery modules, SAE J1798, January 1997.
[25] Effectiveness and Impact of Corporate Average Fuel Economy (CAFE) Standards, Committee on the Effectiveness and impact of Corporate Average Fuel Economy (CAFE) Standards, National Academy Press, Washington, DC, 2001.